DOI: 10.1002/anie.201107907

Tropos Ligands

Effects of the Stationary Phase and the Solvent on the Stereodynamics of biphep Ligands Quantified by Dynamic Three-Column HPLC**

*Frank Maier and Oliver Trapp**

Understanding the influence of the solvent and the stationary phase on chiral compounds is essential to controlling their stereodynamics. Fluctional biaryls with axial chirality, where the barrier is highly sensitive to the substitution pattern,[1] would be a suitable series of compounds to study these effects. Biaryls provide classical examples of atropisomers arising from restricted rotation about a σ bond. Biaryl scaffolds are prominent among the diverse phosphine ligands available for asymmetric catalysis.[2] *o*-Substituted biphenyls are stereochemically labile ("tropos") at ambient temperature,[3] and *o*,*o*′-disubstituted biphenyls are generally so, unless the substituents are bulky.[4,5] Hence the main emphasis in ligand synthesis has been directed to the application of atropos *o*-tetrasubstituted biphenyls that maintain stereochemical integrity over a wide temperature range.[6]

The tropos ligand biphep (2,2′-bis(diphenylphosphino)-biphenyl, **1a**; Scheme 1) was first used in ketone hydrogenation catalysts [P_2N_2Ru] in conjunction with enantiomerically pure diamines.[7] A study of [Pt(binol)] complexes with

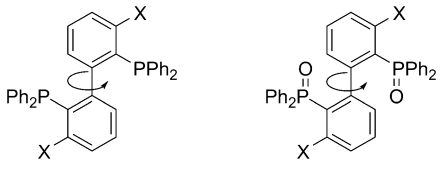

1a (X = H)
1b (X = OMe)
1c (X = O*i*Pr)
1d (X = OBn)

2a (X = H)
2b (X = OMe)
2c (X = O*i*Pr)
2d (X = OBn)

Scheme 1. Structures of investigated biphep ligands.

ligand **1a** by Gagné et al. demonstrated the reduced rate of racemization of the ligand on coordination. The diastereomers of the complex were separated, and the disfavored one was converted into the equilibrium mixture at 90–125 °C, ($\Delta G^{\ddagger} = 123$ kJ mol^{-1} at 382 K). The mechanism of interconversion was left open.[8] Mikami et al. showed that the complexation of biphep by $RuCl_2$ in DMF and reaction with a chiral amine (Scheme 2b) gave only one diastereomer.[9]

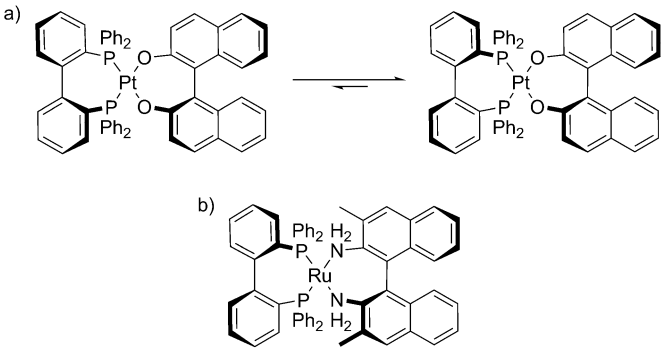

Scheme 2. Early contributions from a) Ref. [9] and b) Ref. [8].

Mikami et al. made further contributions to enantioselective catalysis with **1a**, first by using an enantiopure diamine coligand in Pd complexes.[10a] Removal of the diamine ligand with TfOH gave a stable [(*R*)-**1a**-Pd(MeCN)$_2$](SbF$_6$)$_2$ complex that catalyzed hetero-Diels–Alder reactions.[9b] In situ generation of the analogous Rh complex from **1a** permitted enantioselective ene cyclizations.[10c] A further innovative application involved catalytic asymmetric hydroamination with a cationic **1a**-Au complex, in which an enantiomerically pure counterion was the source of chirality.[11]

The stereointegrity of biphep ligands is crucial in these investigations. There is only a single recorded value for the interconversion of **1a** in the literature, derived by ^{1}H DNMR spectroscopy ($\Delta G^{\ddagger} = 89.5$ kJ mol^{-1} at 125 °C).[12] Therefore an unambiguous method was sought for full characterization of the series.

Enantioselective dynamic HPLC (DHPLC)[4,13] has proved to be a versatile tool for studying the dynamics of interconverting stereoisomers.[14] The enantiomerization barriers $\Delta G^{\ddagger}$ and activation parameters $\Delta H^{\ddagger}$ and $\Delta S^{\ddagger}$ can be determined by evaluation of the elution profiles using the unified equation (see the Supporting Information).[15,16]

Excellent separation of the biphep enantiomers was achieved in presence of the Okamoto type chiral stationary phase (CSP) Chiralpak AD-H[17] with the formation of distinct plateaus caused by rapid interconversion at temperatures between 10 °C and 70 °C. Representative elution profiles of the enantiomers of **1a** and **2a** from the DHPLC experiments are depicted in Figure 1 and the corresponding Eyring plots are shown in Figure 2.

Experimental data for ligands **1a**–**d** and **2a**–**d** determined from the elution profiles are summarized in Table 1. From

[*] Dipl.-Chem. F. Maier, Prof. Dr. O. Trapp
Ruprecht-Karls Universität Heidelberg
Organisch-Chemisches Institut
Im Neuenheimer Feld 270, 69120 Heidelberg (Germany)
E-mail: trapp@oci.uni-heidelberg.de
Homepage: http://www.trapp.uni-hd.de

[**] Generous financial support from the European Research Council (ERC) (Starting Grant No. 258740, AMPCAT, to O.T.) is gratefully acknowledged. We thank Dr. John M. Brown, Oxford University, for the substituted biphep ligands and for helpful discussions.

Supporting information for this article is available on the WWW under http://dx.doi.org/10.1002/anie.201107907.

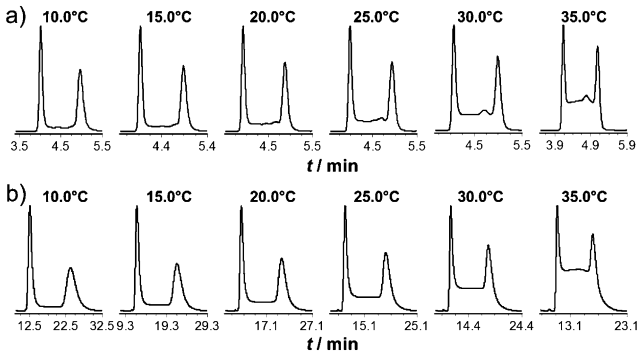

Figure 1. Selected experimental interconversion profiles of a) biphep **1a** and b) biphep=O **2a** obtained by enantioselective DHPLC between 10 °C and 35 °C.

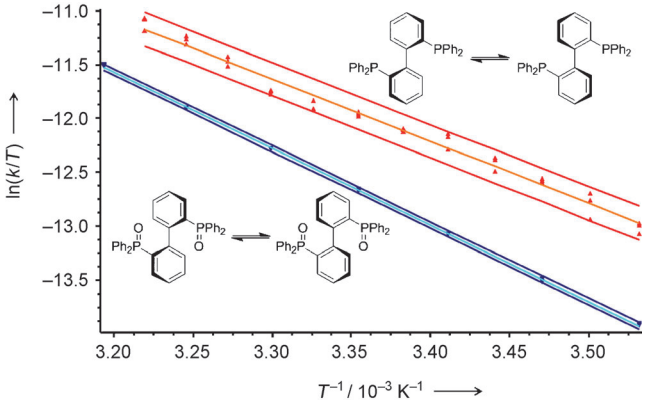

Figure 2. Eyring plot of biphep ligands **1a** and **2a**.

Table 1: Activation parameters obtained by enantioselective DHPLC with a Chiralpak AD-H column.

Entry		$\Delta G^{\ddagger}_{298K}$ [kJ mol^{-1}]	$\Delta H^{\ddagger}$ [kJ mol^{-1}]	$\Delta S^{\ddagger}$ [J mol^{-1} K^{-1}]
1	**1a**	86.8	47.9 ± 0.9	−131 ± 6
2	**1b**	95.3	33.6 ± 1.7	−207 ± 66
3	**1c**	97.0	9.3 ± 0.4	−294 ± 4
4	**1d**	97.1	29.9 ± 2.0	−226 ± 44
5	**2a**	88.6	59.1 ± 0.2	−99 ± 1
6	**2b**	97.2	68.5 ± 0.8	−96 ± 3
7	**2c**	100.4	58.3 ± 1.9	−141 ± 15
8	**2d**	99.7	56.2 ± 1.2	−146 ± 11

these data it is apparent that the Gibbs free energies $\Delta G^{\ddagger}$ of the unsubstituted biphep ligands **1a** and **2a** are lower than those of the 3,3′-disubstituted analogues **1b–d** and **2b–d**; the additional substituents exert a buttressing effect[18] that increases steric hindrance along the reaction coordinate.

These results give a value for the interconversion barrier $\Delta G^{\ddagger}$ of **1a** that is in the range of that determined by Schlosser et al. at far higher temperatures (DNMR, $\Delta G^{\ddagger} = 89.5$ kJ mol^{-1} at 125 °C in 1,1,2,2-tetrachloro[$^2H_2$]ethane, Ref. [12]). The rate of enantiomerization of the biphep ligands **1a** and **2a** at 25 °C was calculated to be 1.8×10^{-3} s^{-1} and 8.9×10^{-4} s^{-1}, respectively.

A comparison of the investigated enantiomerization barriers of the 3,3′-disubstituted phosphines **1b–1d** reveals that the $\Delta G^{\ddagger}$ values show only a small increase for bulkier alkoxy groups. However, there is a significant influence of the substituents on the activation enthalpies $\Delta H^{\ddagger}$ and activation entropies $\Delta S^{\ddagger}$.

In particular, the $\Delta H^{\ddagger}$ values of the 3,3′-disubstituted phosphines **1b–1d** range between 9.3 ± 0.4 kJ mol^{-1} for **1c** to 33.6 ± 1.7 kJ mol^{-1} for **1b**. The enthalpy $\Delta H^{\ddagger}$ for the phosphine oxides **2b–2d** is significantly higher and varies from 56.2 ± 1.2 kJ mol^{-1} for **2d** to 68.5 ± 0.8 kJ mol^{-1} for **2b**. The activation entropy $\Delta S^{\ddagger}$ ranges from −96 ± 3 J mol^{-1} K^{-1} for **2b** to −294 ± 4 J mol^{-1} K^{-1} for **1c**. These negative values indicate increased organization of the substrate or its environment at the transition state. Furthermore it was observed that the interconversion barrier was affected by the solvent. Therefore we determined the activation parameters for different solvent mixtures of *n*-hexane/2-propanol (see Table 2).

Table 2: Solvent influence on $\Delta G^{\ddagger}$, $\Delta H^{\ddagger}$, and $\Delta S^{\ddagger}$.

Entry		*n*-Hexane/ 2-propanol[a]	$\Delta G^{\ddagger}_{298K}$ [kJ mol^{-1}]	$\Delta H^{\ddagger}$ [kJ mol^{-1}]	$\Delta S^{\ddagger}$ [J mol^{-1} K^{-1}]
1	**1a**	99:1	86.8	47.9 ± 0.9	−131 ± 6
2	**1a**	98:2	87.1	46.9 ± 1.0	−135 ± 8
3	**1a**	96:4	87.3	43.0 ± 0.7	−149 ± 9
4	**2a**	70:30	88.6	59.1 ± 0.2	−99 ± 1
5	**2a**	60:40	88.5	51.0 ± 0.4	−126 ± 2
6	**2a**	50:50	88.3	56.1 ± 0.5	−108 ± 2

[a] Solvent ratio (v/v).

Altogether a compensation of the activation parameters $\Delta H^{\ddagger}$ and $\Delta S^{\ddagger}$ is observed,[19] and thus the change in $\Delta G^{\ddagger}$ is small in comparison to the changes in the activation parameters.

Ligand **1a** was investigated at 2-propanol concentrations from 1% to 4% (v/v), and ligand **2a** at 2-propanol concentrations from 30% to 50% (v/v) in *n*-hexane. For **1a**, the overall influence of $\Delta S^{\ddagger}$ on $\Delta G^{\ddagger}$ increased with the 2-propanol concentration, which might be explained by coordination effect of the solvent molecules. For **2a** the maximum influence of $\Delta S^{\ddagger}$ was observed at 40% (v/v) 2-propanol. Owing to compensation of the activation parameters, $\Delta G^{\ddagger}$ changed only by 0.5 kJ mol^{-1} for **1a** and 0.3 kJ mol^{-1} for **2a**, respectively, within the solvent range. These results reinforce the importance of solvent, in addition to reactant structure, in determining $\Delta H^{\ddagger}$ and $\Delta S^{\ddagger}$ in these transformations.

However, beside solvent effects, stationary-phase effects are often discussed. It is a challenging task to quantify the influence of the stationary phase. Furthermore, broadly applicable procedures to access such data are lacking. Here, we present a novel approach to investigate stationary-phase effects by coupling three HPLC columns in line (Figure 3).

The analyte passes through the first column, which separates the enantiomers. The second column contains an achiral support and permits partial re-racemization. Finally in the third column, which contains a chiral stationary phase, the degree of re-racemization can be analyzed accurately. Such an

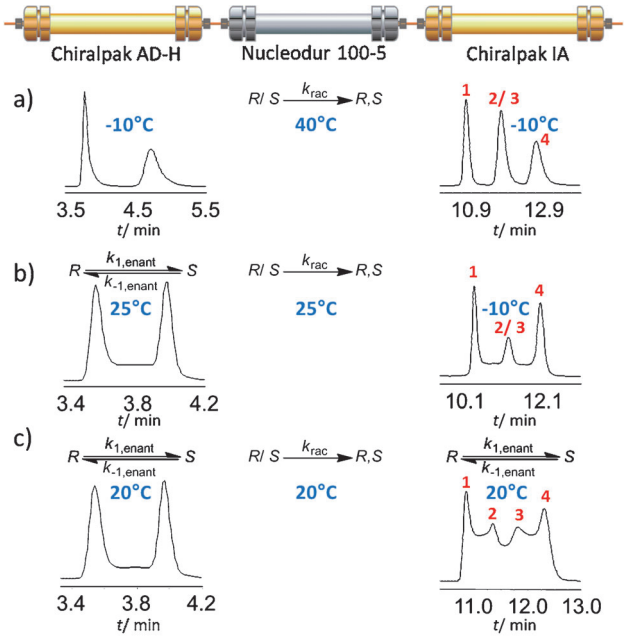

Figure 3. The three-column experimental setup to study enantiomerization and racemization processes and to quantify stationary-phase effects.

arrangement has become feasible by the development of high-pressure-resistant chiral packing materials, which overcome limitations in the solvent back-pressure. With this setup we can simultaneously investigate dynamic and kinetic processes, that is, enantiomerization and racemization, under identical conditions except for the stationary phase.

Depending on the applied temperatures in the respective column sections, elution profiles of varying complexity can be obtained. Consider Figure 3a, where the first and third columns are at lower temperature, and the intermediate achiral column is at an elevated temperature. The elution profile after the second column will be the same as that after the first column, but all analyte molecules will be subject to racemization depending on the reaction time Δt, temperature T, and stationary phase. Passage through the third column separates the de novo enantiomeric mixture, leading to a third peak 2/3 (coincidence of peaks 2 and 3) that is distinct from peaks 1 and 4. The racemization rate constant k_{rac} can be directly calculated from the integrated peak areas and the reaction time [see Eq. (3) in the Supporting Information]. It is important to note that the relation of these two reaction rate constants is $k_{rac} = 2\,k_{enant}$.[20]

Elevation of the temperature of the first column leads to dynamic interconversion profiles in the first column, followed by racemization in the second column. The interconversion of the de novo enantiomeric mixture can be "frozen" by lowering the temperature in the third column (Figure 3b), which makes it possible to independently determine the dynamics (enantiomerization) and kinetics (racemization) in a single experimental setup.

In the case of elevated temperatures in all three columns (Figure 3c), racemization of the separated enantiomers also takes place in the second column, accompanied by simultaneous doubled dynamic interconversion of peaks 1 and 2 (1⇌2), 3 and 4 (3⇌4) (both in the third column), as well as 1 and 4 (1⇌4) (in the first and third columns). Enantiomers of peaks 2 and 3 do not interconvert, because of opposite elution order leading to separation, which reveals the height of the overall plateau, and allows the simultaneous determination of enantiomerization and racemization rate constants.

The power of the method is demonstrated by the results shown in Table 3, for which the surface characteristics of the second column support are varied. Freezing the dynamics in the first and third columns at low temperatures (Figure 3c) gives direct access to racemization kinetics, requiring only minute amounts of racemic mixtures and no preparative separation.

Compared to stopped-flow techniques, the new approach offers many advantages, because perturbations by rapid heating steps to commence isomerization and imprecision in reaction time and temperature are avoided by immediate transfer of the stereoisomers to the second column at elevated temperature. Furthermore, the reaction time is precisely controlled by the flow. The results are summarized in Table 3 and described in detail in the Supporting Information.

Comparison of these data with the data obtained by DHPLC (cf. Tables 1 and 2) reveals an excellent agreement

Table 3: Activation parameters determined by the three-column continuous-flow experiment for the study of stationary-phase effects on the enantiomerization barrier of **1a** (*n*-hexane/2-propanol 99:1, v/v) and **2a** (*n*-hexane/2-propanol 60:40, v/v).

	Solid phase of second column	T_A[a] [°C]	T_B[b] [°C]	T_C[c] [°C]	$\Delta G^{\ddagger}_{298K}$ [kJ mol^{-1}]	$\Delta H^{\ddagger}$ [kJ mol^{-1}]	$\Delta S^{\ddagger}$ [J mol^{-1} K^{-1}]
1a	[d] 	10–35	10–35	−10	87.0	47.9 ± 0.6	−131 ± 5
1a	[d] 	−10	10–50	−10	86.9	47.6 ± 0.3	−132 ± 2
1a	[e] 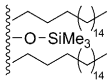	−10	10–50	−10	86.6	33.1 ± 0.3	−179 ± 14
1a	[f] 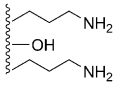	−10	10–50	−10	86.9	47.8 ± 0.8	−131 ± 6
1a	[g] 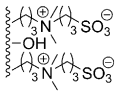	−10	10-50	−10	86.4	42.9 ± 0.6	−146 ± 6
2a	[d] 	−5	10–50	−5	88.0	49.2 ± 0.2	−130 ± 2

[a] Temperature or temperature range of first column (Chiralpak AD-H). [b] Temperature range of second column. [c] Temperature of third column (Chiralpak IA). Chiralpak IA is an immobilized version of Chiralpak AD-H with identical separation properties for the compounds investigated here. [d] Macherey & Nagel Nucleodur 100–5. [e] Merck LiChrospher 100 RP 18e. [f] Macherey & Nagel Nucleodur 100–5 NH_2 RP. [g] Macherey & Nagel Nucleodur HILIC. All measurements were repeated three times each.

with measurements in the presence of neat silica (Nucleodur 100-5).

Surprisingly, $\Delta S^{\ddagger}$ is more negative for the C_{18}-modified silica. It was expected that the apparently deactivated surface exerts no influence. The observed effect can be explained by the hindered rotation of the atropisomers which are aligned parellel to the C_{18} chains. Similar effects were observed in NMR studies by Albert et al.[21]

In summary, we investigated the activation parameters of interconverting tropos biphep ligands and their 3,3′-disubstituted analogues using enantioselective DHPLC in a novel three-column approach. The barriers of 3,3′-disubstituted biphep ligands are significantly higher than those of the unsubstituted ligands as a result of increased steric hindrance. In particular knowing the factors that influence the stereodynamics of ligands is of great importance in the design and understanding of catalysts in asymmetric synthesis. The results clearly suggest that the interconversion process of tropos biphep ligands involve solvent reorganization in the transition state. Our approach, in combination with dynamic chromatography, provides a straightforward, rapid, and highly versatile technique to quantify surface effects, which is normally a challenging and sometimes impossible task. The potential applications of this new technique range from the investigation of surface effects of conformationally labile biomolecules to the quantification of surface-induced self-amplifying processes.

Received: November 9, 2011
Revised: January 3, 2012
Published online: February 9, 2012

Keywords: atropisomerism · biaryls · dynamic HPLC · ligand design · phosphane ligands

[1] G. Bringmann, A. J. P. Mortimer, P. A. Keller, M. J. Gresser, J. Garner, M. Breuning, *Angew. Chem.* **2005**, *117*, 5518 – 5563; *Angew. Chem. Int. Ed.* **2005**, *44*, 5384 – 5427.
[2] R. Noyori, *Angew. Chem.* **2002**, *114*, 2108 – 2123; *Angew. Chem. Int. Ed.* **2002**, *41*, 2008 – 2022.
[3] a) A. Mazzanti, L. Lunazzi, M. Minzoni, J. E. Anderson, *J. Org. Chem.* **2006**, *71*, 5474 – 5481; b) D. Casarini, L. Lunazzi, M. Mancinelli, A. Mazzanti, C. Rosini, *J. Org. Chem.* **2007**, *72*, 7667 – 7676; c) R. Ruzziconi, S. Spizzichino, A. Mazzanti, L. Lunazzi, M. Schlosser, *Org. Biomol. Chem.* **2010**, *8*, 4463 – 4471.
[4] a) C. Wolf, *Dynamic Stereochemistry of Chiral Compounds, Principles, Applications*, RSC Publishing, Cambridge, **2008**, chap. 3, p. 29; b) C. Wolf, *Chem. Soc. Rev.* **2005**, *34*, 595 – 608; c) C. Wolf, H. Xu, *Tetrahedron Lett.* **2007**, *48*, 6886 – 6889; d) C. Wolf, W. A. König, C. Roussel, *Chirality* **1995**, *7*, 610 – 611.
[5] Some exceptions: a) C. Wolf, D. H. Hochmuth, W. A. König, C. Roussel, *Liebigs Ann.* **1996**, 357 – 363; b) C. Wolf, W. A. König, C. Roussel, *Liebigs Ann.* **1995**, 781 – 786; c) A. Patti, S. Pedotti, *Tetrahedron: Asymmetry* **2005**, *16*, 965 – 970; d) P. U. Biedermann, V. Schurig, I. Agranat, *Chirality* **1997**, *9*, 350 – 353; e) V. Schurig, S. Reich, *Chirality* **1998**, *10*, 316 – 320.
[6] Tropos, atropos reviewed: K. Mikami, K. Aikawa, Y. Yusa, J. J. Jodry, M. Yamanaka, *Synlett* **2002**, 1561 – 1578.
[7] K. Mikami, T. Korenaga, M. Terada, T. Ohkuma, T. Pham, R. Noyori, *Angew. Chem.* **1999**, *111*, 517 – 519; *Angew. Chem. Int. Ed.* **1999**, *38*, 495 – 497.
[8] M. D. Tudor, J. J. Becker, P. S. White, M. R. Gagné, *Organometallics* **2000**, *19*, 4376 – 4384.
[9] K. Mikami, K. Aikawa, T. Korenaga, *Org. Lett.* **2001**, *3*, 243 – 245.
[10] a) K. Mikami, K. Aikawa, Y. Yusa, *Org. Lett.* **2002**, *4*, 95 – 97; b) K. Mikami, K. Aikawa, Y. Yusa, M. Hatano, *Org. Lett.* **2002**, *4*, 91 – 94; c) K. Mikami, S. Kataoka, Y. Yusa, K. Aikawa, *Org. Lett.* **2004**, *6*, 3699 – 3701.
[11] K. Aikawa, M. Kojima, K. Mikami, *Angew. Chem.* **2009**, *121*, 6189 – 6193; *Angew. Chem. Int. Ed.* **2009**, *48*, 6073 – 6077; K. Mikami, H. Kakuno, K. Aikawa, *Angew. Chem.* **2005**, *117*, 7423 – 7426; *Angew. Chem. Int. Ed.* **2005**, *44*, 7257 – 7260.
[12] O. Desponds, M. Schlosser, *Tetrahedron Lett.* **1996**, *37*, 47 – 48.
[13] a) O. Trapp, G. Schoetz, V. Schurig, *Chirality* **2001**, *13*, 403 – 414; b) J. Krupcik, P. Oswald, P. Majek, P. Sandra, D. W. Armstrong, *J. Chromatogr. A* **2003**, *1000*, 779 – 800; c) I. D'Acquarica, F. Gasparrini, M. Pierini, C. Villani, G. Zappia, *J. Sep. Sci.* **2006**, *29*, 1508 – 1516.
[14] a) M. Jung, V. Schurig, *J. Am. Chem. Soc.* **1992**, *114*, 529 – 534; b) O. Trapp, V. Schurig, *J. Am. Chem. Soc.* **2000**, *122*, 1424 – 1430.
[15] a) O. Trapp, *Anal. Chem.* **2006**, *78*, 189 – 198; b) O. Trapp, *Chirality* **2006**, *18*, 489 – 497; O. Trapp, S. K. Weber, S. Bauch, W. Hofstadt, *Angew. Chem.* **2007**, *119*, 7447 – 7451; *Angew. Chem. Int. Ed.* **2007**, *46*, 7307 – 7310; c) O. Trapp, S. Bremer, S. K. Weber, *Anal. Bioanal. Chem.* **2009**, *395*, 1673 – 1679; d) J. Troendlin, J. Rehbein, M. Hiersemann, O. Trapp, *J. Am. Chem. Soc.* **2011**, *133*, 16444 – 16450.
[16] O. Trapp, *J. Chromatogr. B* **2008**, *875*, 42 – 47.
[17] Y. Okamoto, E. Yashima, *Angew. Chem.* **1998**, *110*, 1072 – 1095; *Angew. Chem. Int. Ed.* **1998**, *37*, 1020 – 1043.
[18] M. Rieger, F. H. Westheimer, *J. Am. Chem. Soc.* **1950**, *72*, 19 – 28.
[19] J. D. Dunitz, *Chem. Biol.* **1995**, *2*, 709 – 712.
[20] M. Reist, B. Testa, P.-A. Carrupt, M. Jung, V. Schurig, *Chirality* **1995**, *7*, 396 – 400.
[21] M. Raitza, J. Wegmann, S. Bachmann, K. Albert, *Angew. Chem.* **2000**, *112*, 3629 – 3632; *Angew. Chem. Int. Ed.* **2000**, *39*, 3486 – 3489.

